

An Optical Method for In Situ Characterization of Fouling During Filtration

J. Mendret, C. Guigui, P. Schmitz, and C. Cabassud

UMR5504, UMR792 Ingénierie des Systèmes Biologiques et des Procédés, CNRS, INRA, F-31400 Toulouse, INSA, 135 avenue de Rangueil, 31 077 Toulouse cedex 4, France

P. Duru

UMR CNRF-INP-UPS 5502, Institut de Mécanique des Fluides de Toulouse, allée du Professeur Camille Soula, 31 400 Toulouse, France

DOI 10.1002/aic.11257

Published online July 27, 2007 in Wiley InterScience (www.interscience.wiley.com).

In dead-end ultrafiltration, in situ characterization of fouling is of great importance to be able to evaluate cake properties during filtration runs. Moreover, local information is necessary to analyze and model the basic mechanisms involved in deposit formation. Many studies have investigated cake formation on flat-sheet membranes but there is a lack of methods suitable for confined geometries such as inside-out hollow-fiber membranes. This study focuses on development and validation of an optical method using a laser sheet for in situ cake characterization in a narrow channel. The method enables the measurement of time-variations of cross-section cake thickness ranging from 10 μm to hundreds of micrometers with a 3 μm resolution and a 2.5 μm standard deviation. The reproducibility of the results and the order of magnitude are discussed on the basis of experimental results for clay suspensions. Limitations of the method are investigated; in the range of 0–2 g/l for clay suspensions, suspension concentration has no effect. Finally, future applications of the method as a tool for dead-end fouling characterization are considered. © 2007 American Institute of Chemical Engineers AICHE J, 53: 2265–2274, 2007

Keywords: *in situ measurement, membranes, optical method, particle fouling, hollow-fiber, dead-end ultrafiltration*

Introduction

Ultrafiltration (UF) with hollow-fiber membranes is widely used in drinking water production or wastewater treatment for their ability to remove particles, colloidal species, and microorganisms from different liquid feeds.¹ Nowadays, dead-end filtration is the only viable mode as it enables power consumption to be minimized. However, a limitation inherent in the process is the high and rapid membrane fouling because of the continuous arrival of suspended matter during filtration. Thus, backwash operations are periodically

required for fouling removal but some recent studies have shown that the estimation of their efficiency is difficult as some remaining fouling cannot be detected easily through the measurement of flux recovery.² Therefore the understanding of formation and transport properties of particle deposit responsible for membrane fouling is a necessary step in the optimization of dead-end UF processes with inside-out hollow-fiber membranes.

Using basic filtration laws it is possible to estimate global parameters such as irreversible and specific cake hydraulic resistances, from flow rate and pressure measurements during operation. Those laws assume monodisperse particles, homogeneous properties of the deposit on the membrane surface and uniform flow rate. However, local variables such as thickness and porosity of the cake are difficult to obtain.

Correspondence concerning this article should be addressed to J. Mendret at Julie.mendret@insa-toulouse.fr.

Nonetheless, local information is necessary to analyze and model the basic mechanisms involved in deposit formation to further predict process operation. Most of the time, local measurements are performed *ex situ* after sampling. In this case, the deposit structure may be modified by the pressure-release and a possible cake dislocation during sampling. The only way to obtain local information about the deposit structure at a given time during filtration is to use an *in situ* and real-time measurement with a noninvasive method, that is to say, which does not disturb the process and cake build-up during filtration or removal during hydraulic cleanings.

This article focuses on the development of a new method to characterize *in situ* particulate fouling at local scale during dead-end UF. The method is especially dedicated to confined geometries. First, a review is given about the different noninvasive methods to characterize membrane fouling that have already been proposed in the literature. A careful presentation and discussion is proposed in terms of application domain, complexity, benefits, and drawbacks. Second, the principle of the original method proposed in this article is detailed. Finally, this method is applied and validated for dead-end filtration of clay suspension in a narrow channel with one membrane wall. Moreover, some future possible applications will be discussed for this innovative method.

Noninvasive Characterization Methods of Membrane Fouling

Over the last few years, a number of noninvasive techniques have been used to observe *in situ* membrane processes.^{3,4} In this section the methods which can enable the detection of a surface deposit from a few micrometers thickness are presented and discussed.

Direct observation through the membrane/direct observation above the membrane

Direct observation through the membrane (DOTM) is a method which enables the visualization of the deposit first layer formation. This technique is based on the use of a microscope objective positioned at the permeate side of a transparent membrane. When this special membrane is wet, it becomes transparent and a glass window on the module enables particle deposition to be observed. Li et al.⁵ used this technique to estimate the critical flux (the flux which leads to the first layer formation) and to study deposition of latex particles (particle diameter (d_p) of 3.0, 6.4, and 11.9 μm) above and below this critical flux. Membranes were Anopore (Whatman, UK) and Millipore Teflon. Flux decrease was related to the percentage of membrane area covered by the deposit (obtained by image analysis). DOTM is particularly suitable for particles larger than 1 μm and can also be applied to sub-micron particles using fluorescence microscopy. This technique is a powerful tool for studying the initial step of deposit formation and of membrane/particles interactions (influence of pH, ionic strength, and so on) but the observation is limited to the first layer of the deposit. Furthermore, the technique requires the use of specific membranes, which are very fragile and need care. Moreover, it is quite qualitative.

Direct visualization above the membrane (DVAM) is a similar technique which enables the dynamics of cake build-

up and removal to be followed. It consists of a microscope positioned in the feed side of the module. Mores and Davis⁶ could observe the deposition and removal of yeast particles (*Saccharomyces cerevisiae*) on cellulose-acetate and Anopore anodised alumina membranes. This technique does not require a membrane as transparent as that for DOTM but the feed solution has to be clear enough.

Those methods offer a good resolution (0.5 μm) but are difficult to use to estimate cake thickness.

Confocal laser scanning microscopy

Confocal laser scanning microscopy (CLSM) is a valuable tool for obtaining high resolution images, termed optical sections, and 3D reconstructions. This technique has a better resolution than conventional fluorescence as it reduces the background information away from the focal plane (that leads to image degradation). In a laser scanning confocal microscope, a laser beam passes a light source aperture and is then focused by an objective lens into a fluorescent specimen. Some macromolecules present autofluorescence or have an inherent fluorescent capacity but most of the time fluorescence has to be induced by a chemical treatment. The specimen is scanned pixel by pixel and the emitted fluorescent light is collected by a photomultiplier, which transforms the light signal into an electrical one. This signal intensity depends on the number of photons received by the photomultiplier; it is then digitized in a grey level intensity. Concerning fouling characterization in membrane processes, CLSM was especially used for the study of protein adsorption. Ferrando et al.⁷ worked on the characterization of fouling during microfiltration of single and binary protein solutions by CLSM. They were able to estimate the fraction of pore surface in which proteins were detected in relation to the permeate flux. The 3D reconstruction is useful for visualizing the distribution of the fouling agents inside the membrane. One of the main advantages of CLSM over other characterization methods is that it allows different species to be distinguished (depending on their fluorescent emission) and on-line adsorption and desorption processes at different depths in the membrane to be visualized. Nonetheless, it becomes difficult to use for multiple proteins as several labels have to be used in addition to the label required for the membrane. Moreover, there is a possibility that the label used may affect the physicochemical and adsorption properties of the proteins. The main limitation of the method is related to its resolution and penetration depth. In the best case, the CLSM resolves 180 nm in the focal plane and 400–800 nm along the optic axis (this corresponds to the thickness of an optical slice). Therefore, for surface characterization, it is limited to microfiltration membranes. Finally, the penetration depth is quite small (about 50 μm in the best cases) and corresponds to the maximum observable thickness.

Optical laser sensor

With an optical laser sensor it is possible to measure a deposit thickness during filtration. The method is based on the use of a laser beam, which is focused tangentially to the surface of a tubular membrane. The image of the focused point is then captured by a photomultiplier, which measures the signal intensity. At the beginning of the filtration the energy

collected by the photomultiplier is maximum and then it decreases as the deposit grows and absorbs the signal. Thus the intensity variation is directly related to the deposit thickness. A calibration curve enables the instantaneous signal magnitude to be associated to the deposit thickness. When all the signal intensity is absorbed, no more light is detected by the photomultiplier, which determines the maximum cake thickness that can be measured. Hamachi et al.⁸ performed a dynamic measurement of the deposit thickness using an optical He–Ne laser sensor ($\lambda = 543.5$ nm, 0.2 mW) during microfiltration of clay suspensions ($d_p = 2.45$ μm) with an outside-in tubular membrane. They used a module with two glass windows. Thus deposit thickness measurements were performed at a single position, between the inlet and the outlet of the tubular membrane, assuming that the point is representative of the global deposit growth. The maximum cake thickness they could measure was 30 μm but they overcame this limitation by moving the sensor 30 μm away with a micrometric screw device. This displacement takes only a few seconds so that recording was considered as continuous. However, with this technique, there is a maximum possible concentration for the suspension (375 mg/l for Hamachi et al.) above which the laser beam intensity is totally absorbed by suspended particles.

Photointerrupt sensor

When an object is close to a photointerrupt sensor, the light from the emitter (high-intensity infrared LED, $\lambda = 950$ nm) is reflected from the surface of the object into the collector (high-gain silicon photo-Darlington transistor). Decreasing the distance between the object and the sensor results in an increase in reflective current. Tung et al.⁹ applied this method to follow the deposit thickness growth during cross-flow filtration of PMMA particles ($d_p = 5.15$ μm). They tested the influence of several parameters on the accuracy of the measurement: sample color, slurry concentration, stirred rate, etc. Increase in slurry concentration disturbs the measurement because of the attenuation of the signal to the collector due to the dispersion of the light by the suspended particles. With PMMA suspension, the maximum error in thickness measurement is less than $\pm 6.29\%$ for slurry concentrations below 1% (w/w). Moreover, the deposit color (or slurry color) is a major problem: when an IR light passes through a colored object, some IR wavelengths are readily absorbed and cause the reduction in photocurrent back to the collector. However, the authors add that deposit color is always the same for specified filtration slurry so that this effect can be eliminated after calibration. Nevertheless, some preliminary tests performed in our laboratory with this method showed that problems can occur if the membrane and the slurry are of different colors. Tung et al.⁹ measured cake thickness ranging from 10 μm to 5 mm with a 10 μm resolution. This method has the benefits of being cheap and easy to install and offers good accuracy, but it is also very sensitive to color parameters and more suitable for dilute suspensions than for concentrated suspensions.

Nuclear magnetic resonance imaging

Nuclear magnetic resonance (NMR) imaging is usually associated to the medical sector as a noninvasive means of

obtaining clinical images and of studying tissue metabolism *in vivo*. For a decade it has been extended to other areas like flow visualization and deposit characterization in membrane processes.³ Nuclei with an odd number of protons and neutrons have a property called spin, which can be visualized as a rotating motion of the nucleus around its own axis. As atomic nuclei are charged, the spinning motion causes a magnetic moment in the direction of the spin axis. The strength of the magnetic moment is a property of the type of nucleus: hydrogen nuclei possess the strongest magnetic moment. Initially individual moments have random orientation. When a magnetic field is applied, they align themselves parallel or antiparallel with respect to the applied magnetic field. Resonance is caused by the application of a radio frequency magnetic field that changes proton alignment. The return from their excitation state induces a signal received by the coil of the apparatus. The intensity of this signal is proportional to the number of protons in the sample. Each voxel of the sample resonates with a specific frequency; a NMR imaging is a matrix of signal intensity from the nuclei of the sample. With this method, a resolution of 10 μm and below can be obtained. Samples must suit with the magnetic coil diameter (up to 30 cm). In membrane processes, NMR imaging was used for the study of flow distribution in tubular and hollow-fiber modules.¹⁰ Wandelt et al.^{11,12} applied this method *in situ* to investigate deposit growth during cross-flow microfiltration of clay ($d_p = 0.8$ μm) suspensions. Clay deposit had no spin population and made a black area near the membrane surface on the NMR images. The deposit formation and removal can be studied from image analysis. Furthermore, this method can be used to study the deposit compressibility. Indeed, by increasing the pressure in steps and taking images after each step, it is possible to measure the deposit thickness as a function of the pressure. NMR imaging shows many interesting aspects (good resolution, nondestructive, enables flow analysis, etc.) but yet to be fully applied to membrane processes. The major drawback of NMR is its high device specificity level and the difficulty of extracting an optimal information and of evaluating artefacts generated by cake growth. Moreover the time to process an image is long (about 15 min in the experiments of Wandelt).

Small-angle neutron scattering

Small-angle neutron scattering (SANS) is a nondestructive method for the determination of microstructures. It is based on the principle that an initially parallel neutron beam is scattered by heterogeneities of a sample. These can be due to fluctuations in density, concentration, or magnetization. The resulting scattering pattern can be analyzed to provide information about size, shape, and orientation of the components of the sample. In comparison with X-rays, neutrons have weak interactions with matter and thus are highly penetrating. Pignon et al.¹³ used SANS for the *in situ* structural characterization of deposits formed during dead-end filtration of Laponite XLG ($d_p = 30$ nm) suspensions. When the observation distance from the membrane was decreased, they noticed an anisotropic increase in scattering intensity in the deposit that gives information about the distance between particles and the orientation of the particles through the deposit. Because of the strong penetration capability of neutrons,

SANS enables a characterization in various geometries with long path lengths (like membrane modules), on condition that the material is transparent to neutron (alumina, silica, quartz) and samples are lab-scale sized. Moreover it offers very good resolution (from 0.1 nm to around 10 nm). However, this method requires highly specific equipment and a specialist support to extract information about the cake structure from scatter results.

Ultrasonic reflectometry

Ultrasonic time-domain reflectometry (UTDR) uses sound waves to measure the position of a moving interface and could provide information on the physical characteristics of the media through which the waves propagate. When ultrasonic waves encounter an interface between two media, energy is partitioned in such a way that a reflected wave occurs, which can be detected by an ultrasonic transducer. The amplitude and the time of flight of the reflected wave relative to the incident wave are determined by the acoustic impedance difference between the two media and the topography of the surface. Li et al.¹⁴ applied this method to characterize bovine serum albumine (BSA) layers obtained during UF on polysulfone membranes. They found a good relationship between the ultrasonic signal response and the development of BSA gel layer on the membrane surface. They were able to estimate cake thickness (of about 30 μm) using the difference in arrival time between the signal on a fouled membrane and the signal on a clean membrane. Because of the lack of knowledge about the propagation mode of an acoustic wave in a deformable deposit, amplitude measurements can only provide qualitative characterization of the cake formation process. Investigation on the acoustic propagation is in progress and will enable a structure analysis to be made.¹⁵ UTDR is a promising technique provided that the propagation of acoustic waves in particle deposits is better known, which requires further investigations. Moreover, it is one of the few noninvasive methods potentially applicable to commercial-scale modules.

Laser triangulometry

In contrast to the optical laser sensor method developed by Hamachi et al., laser triangulometry is an optical method based on the reflection of a laser beam from a surface whose position varies, like a developing particle layer. A CCD camera is used to capture the reflected beam. As the deposit grows, the reflected beam shifts and the measurement of this shift allows the calculation of the deposit thickness. Altmann and Ripperger¹⁶ studied the particle deposition and the layer formation during cross-flow microfiltration of diatomaceous earth and silica particles with a commercial laser triangulometer. The cake layer height was measured in situ through a transparent window on the membrane module. This method enables deposit thickness to be measured in real-time and offers good resolution (5 μm), depending on the camera and objective's own resolution.

Conclusion

As can be seen in the synthesis and comparison of the methods given in Table 1, UTDR and NMR can be applied with all kind of materials, whereas, for other techniques, the

filtration module must have a glass window or must be transparent to neutrons.

The average resolution of those techniques is between 0.5 and 10 μm except for SANS, which enables the nanostructure of the deposit to be studied.

Optical laser sensors, photo-interrupt sensors, UTDR, and laser triangulometry enable the cake thickness growth to be followed in real time. DOTM, DVAM, and CLSM are valuable tools to study the interactions between membrane and particles. Finally, SANS and UTDR can provide information about the deposit structure.

The literature review shows that a number of in situ and noninvasive techniques can be used to study cake layer formation on plane geometry, however, few studies concern fouling characterization in a confined geometry such as a hollow fiber, except for NMR imaging which is very restrictive because of the highly specific equipment. In this context, the aim of this study is to develop and validate an in situ fouling characterization method, suitable for a confined membrane geometry and relatively easy to carry out. The mid-term objective is to use this method to understand fundamental mechanisms involved in deposit formation and removal in relation to filtration or cleaning operating parameters.

Laser triangulometry is an interesting method but enables characterization in only one single point (equivalent to the laser beam surface). The method presented in this article is inspired from laser triangulometry but is based on the use of a laser sheet that allows a larger characterization surface for deposit thickness measurements and enables the examination of deposit thickness in the cross-section.

Materials and Principle of the Developed Method

Filtration module

Our goal is to develop an experimental technique able to characterize fouling in a confined geometry. A narrow rectangular channel with one membrane wall was designed (Figure 1). This geometry (length = $15 \times$ width) introduces some confinement effects similar to those occurring in an inside/out hollow-fiber and allows to observe their influence on the deposit build-up. Also, a geometry with such small dimensions imposes some constraints on the experimental technique, which have to be coped with.

Each of the two parallel plates of a flat transparent Plexiglas chamber was machined with a 28.2 cm height and 2 mm large and depth channel. A flat-sheet membrane [Polysulfone, Molecular weight cut off (MWCO) = 100 kDa] was put between the two plates; thus filtration is operated only on one channel wall ($56.4 \times 10^{-5} \text{ m}^2$ of effective filtration area). This filtration device is operated in dead-end at constant transmembrane pressure (TMP). Liquid feed can be introduced from the bottom or from the top of the channel. Each of the two plates was connected to a piping network that enables to operate filtration (Figure 2).

An electronic balance connected to a PC enables the permeate mass versus time to be acquired to measure the permeate flux time variations. For each experiment, a new membrane was used and its initial permeability was measured with pure water. The initial permeability of the polysulfone membranes was in the range 1.8–2.5 l/h m^2 kPa at 20°C.

Table 1. Synthesis and Comparison of Noninvasive Methods for Fouling Characterization

| Method | Specific Membrane or Module | Resolution | Complexity of the Equipment | Applied to | Benefits | Drawbacks |
|---------------------------------------|---|-----------------------|-----------------------------|--|--|---|
| DOTM ⁵ | Anapore or Millipore Teflon membrane/module with a glass window | >0.5 μm | Low | f.s. membrane/latex ($d_p = 3, 6.4, 11.9 \mu\text{m}$) | Membrane/particles interactions study | Limited to the first layer, fragile membrane |
| DVAM ⁶ | Glass window | >0.5 μm | Low | f.s. membrane/yeast particles fluorescent latex | Dynamic of cake layer build-up/removal | Only for dilute suspensions |
| CLSM ⁷ | Transparent module | 180 (xy), 400–800 (z) | Moderate | Adsorption/desorption of protein on f.s. membrane | Can distinguish different species | Complex when too many labels, small penetration depth |
| Optical laser sensor ⁸ | Glass window | 10 μm | Low | Outside-in tubular membrane/bentonite ($d_p = 2, 45 \mu\text{m}$) | Real-time cake thickness | Maximum possible concentration |
| Photo-interrupt ⁹ | Transparent module | 10 μm | Low | f.s. membrane/PMMA particles ($d_p = 5.15 \mu\text{m}$) | Real-time cake thickness, inexpensive, easy installation | Sensitive to color parameters |
| NMR ^{10–12} | Module diameter <30 cm | 10 μm | High | Inside-out h.f./bentonite ($d_p = 0.8 \mu\text{m}$), oil-water emulsions, silica ($d_p = 10 \text{ nm}$) | Non invasive, applicable to h.f. | Require specialist support |
| SANS ¹³ | Material transparent to neutrons | 0.1 nm | High | f.s. membrane/protein laponite XLG ($d_p = 30 \text{ nm}$) | High resolution, noninvasive (applicable to h.f.) | Require specialist support |
| UTDR ^{14,15} | – | 5–10 μm | Moderate | f.s. and tubular membrane/ CaSO ₄ , BSA, paper mill effluent, kaolin ($d_p = 2 \mu\text{m}$) | Information about physical parameters and cake thickness | Lack of knowledge on acoustic wave propagation |
| Laser triangulometry ^{16,17} | Transparent module | 5 μm | Low | f.s. membrane/diatomaceous earth, silica particles, fluorescent latex | Real-time cake thickness, good resolution | Concentration limitation |

f.s., flat-sheet; h.f., hollow fiber.

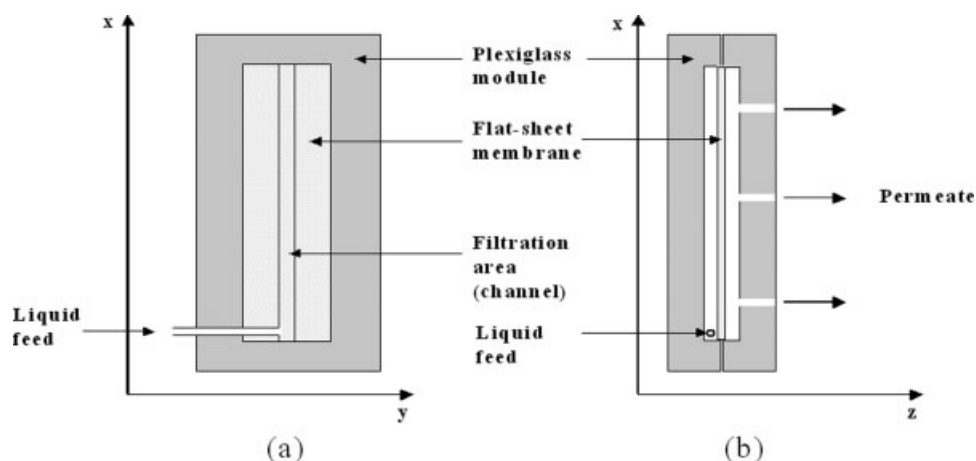


Figure 1. Filtration module: (a) front view (if the feed flows from the bottom of the channel), (b) side view (cutaway in the channel).

Principle of the deposit thickness measurement with laser sheet at grazing incidence

The principle of the experimental technique we developed to measure the deposit thickness is similar to the one of laser triangulometry. In our experiment, a laser sheet is positioned at grazing incidence relative to the filtration module (Figure 3a) and is focused on the membrane. The laser sheet is obtained using a Lasiris SNF-501L laser diode (power 3.5 mW and wavelength 635 ± 5 nm) and a specific lens positioned at the laser diode output. The impact line is perpendicular to the x -direction and is larger than the channel width. A CCD camera (cooled digital 12 bit Sencicam QE camera, with captor size $1376 \text{ pixels} \times 1040 \text{ pixels}$) records the laser light reflected by the membrane in the direction perpendicular to the membrane.

The part of the laser sheet which is reaching the membrane outside of the channel undergoes a single refraction along its path before reaching the membrane, at the interface between air and Plexiglas (Figure 3b). The part of the laser sheet which is reaching the membrane inside the channel undergoes two refractions: at the interface between air and Plexiglas and at the interface between Plexiglas and water (Figure 3b). Consequently, there is a shift between the positions of the laser line outside and inside the channel because of the refractive index difference. When a deposit is growing during a filtration experiment, the laser light is reflected at its surface and consequently, the measured shift ΔX decreases with time (Figure 3b). The shift evolution as a function of time, $\Delta X(t)$, is measured on the video images.

The deposit thickness at time t , $e_d(t)$, is given by the following relationship:

$$e_d(t) = \frac{\Delta X(t) - \Delta X(t=0)}{\tan \theta_3} \quad (1)$$

The shift at $t = 0$, when there is no deposit, is related to the channel height and to the angles θ_2 and θ_3 by the relation:

$$\Delta X(t=0) = h \cdot (\tan \theta_3 - \tan \theta_2) \quad (2)$$

where h is the channel height. The relation between θ_2 and θ_3 is given by Snell–Descartes's law:

$$n_2 \cdot \sin \theta_2 = n_3 \cdot \sin \theta_3 \quad (3)$$

where n_2 and n_3 are, respectively, the refractive indexes in Plexiglas and in water with values of 1.5 and 1.33, respectively. Then, Eq. 2 can be written:

$$\Delta X(t=0) = h \cdot \left[\tan \theta_3 - \tan \left[\arcsin \left(\frac{n_3}{n_2} \cdot \sin \theta_3 \right) \right] \right] \quad (4)$$

Resolution of Eq. 4 allows to get θ_3 from the measurement of $\Delta X(t=0)$.

Image analysis

A typical image obtained by the CCD camera is presented in Figure 4. Images are processed using the software Matlab. Various regions of interest (ROI) can be selected on a given image.

One can then obtain averaged intensity profiles of the reflected light for the various ROI, the averaging being performed over the width (y -direction) of each ROI. Such light intensity plots present a clear maximum (Figure 4), the existence of which is related to the fact that the incident light intensity profile is Gaussian over the width of the laser sheet. The shift ΔX is found by measuring the difference between the position of the maximum intensity of the reflected light

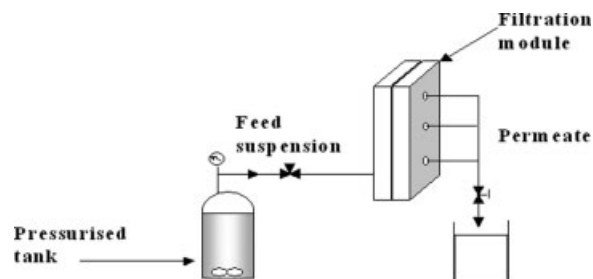


Figure 2. Experimental set-up.

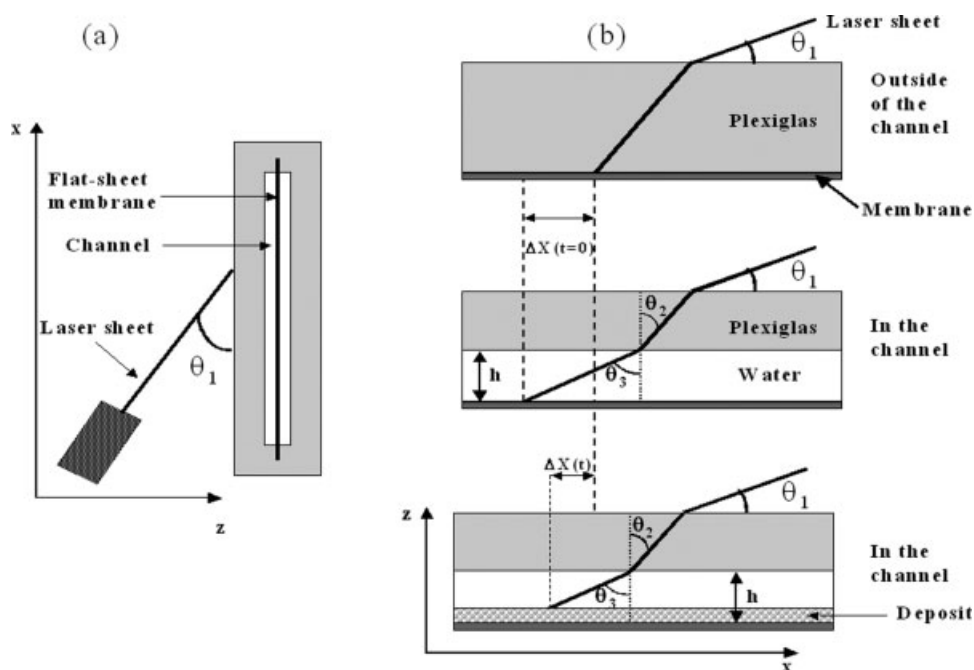


Figure 3. Laser deflections in the module.

(a) Position of the laser sheet, (b) deflection of the laser outside of the channel (top figure) and inside the channel (bottom figure).

on a given ROI in the channel (for instance, ROI 1 on Figure 4) and the position of the maximum intensity of the reflected light in a reference area outside of the channel (ROI 2 on Figure 4). The position of the maximum, in pixel, is obtained the following way: the intensity profiles are first fitted with a sum of quartic B-spline function, over 10 subintervals. Then, the x -position of the maximum of this analytical function is

determined (Figure 4). This fitting step is necessary to smooth the experimentally found intensity profiles, which are slightly noisy despite the transverse averaging. For the given optical set-up and image acquisition system, the minimum width of the ROI allowing such a fit to find a clear maximum was 10 pixels, which gives the transverse resolution that can be achieved by this technique.

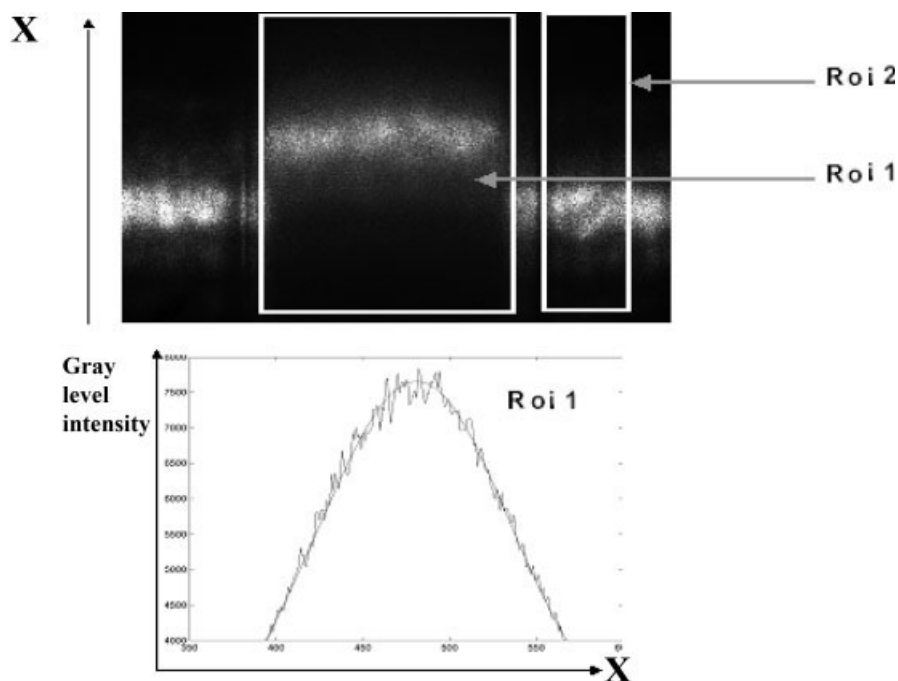


Figure 4. Plot of the gray level intensity and determination of the position of the maximum for a region of interest.

Measuring ΔX and $\Delta X(t = 0)$ enables the cake thickness $e_d(t)$ to be determined using Eq. 1. The switch from pixels to length is done using an image of the channel without the laser sheet, using the fact that the channel is 2 mm wide.

Capabilities and limitations of the presented experimental technique

Compared to the laser triangulometry technique, the originality of this technique lies in the use of a thin laser sheet instead of a crude laser spot. Consequently, measurements of deposit thickness profiles in the direction transverse to the channel can be obtained by dividing the channel in several ROIs as explained earlier. The lateral resolution of our technique is defined by the minimum lateral size of the ROIs that can be used, which is 25 micrometers with the magnification used in this study. However, it must be noted that it is not possible to obtain an accurate thickness value near the channel wall because of the signal being too noisy, probably due to light diffusion from the wall.

One can also consider to move the set laser-camera in the x -direction to measure the deposit thickness at different x positions. As the laser sheet thickness is small, one could expect a good spatial resolution in the x -direction. Finally, this would allow to get a deposit thickness “map” as a function of x and y . It must be mentioned that in the present experimental device, the optical setting were tricky so that displacement in the x -direction during an experiment was not easy and measurements were performed at a given x .

The accuracy in thickness measurement is on one hand determined by the accuracy of the measurement of the difference $\Delta X(t) - \Delta X(t = 0)$ which is estimated to be ± 2 pixels. On the other hand, another uncertainty happens when converting from pixel to mm as the measurement of the exact channel width is difficult to estimate. Indeed, this measurement is tricky because of parallax effects and light diffusion from the lateral walls. The latter effect is due to wall surface roughness: it cannot be avoided but may be reduced by polishing the channel walls. We estimate the uncertainty on the channel width determination to be ± 4 pixels. It could be lowered by using a larger CCD array and larger magnification for the optics. The resulting global uncertainty on the cake thickness measurement is estimated to be $\pm 2.5 \mu\text{m}$.

The minimum cake thickness that can be measured with this technique is estimated to be $3 \mu\text{m}$. This measurement resolution is limited by the pixel resolution of the CCD sensor and the zoom lens capability. It could be made more accurate by using a smaller angle θ_3 ($\theta_3 = 50^\circ$ in this study). However, a $3 \mu\text{m}$ resolution is good in comparison with the other characterization methods (Table 1).

This experimental technique also allows the deposit growth to be characterized versus time by applying the method presented earlier for successive images and thus the cake growth kinetics to be obtained. In this study, the image acquisition rate was low (typically one frame per minute) but it could be much larger (up to a few images per seconds with the acquisition system used) so that this measurement technique could be used for much more rapid membrane fouling.

Like many optical methods, the method presented in this article is limited by the concentration of the suspension.

Indeed, at large concentration, light diffusion by the suspended particles is going to “blur” the image of the laser sheet. In this study, concentrations of 1 g/l and 2 g/l were tested for clay suspensions. In both cases, image processing allowed the determination of a sharp maximum in the light intensity profile and thus the deposit thickness measurement was possible. Higher concentrations will be tested but it seems that the method is well suited to a range of concentrations corresponding to those encountered in drinking water production and that the range of concentration for which the technique is usable is larger than for other techniques.

Application and Validation for a Given Example

Some typical results: filtration of clay suspensions

It has been seen in the previous section that the developed method enables the flow rate of permeate and the deposit thickness to be measured simultaneously for several locations along the channel length. For a fixed x position, it is possible:

- to determine the deposit kinetics (cake growth thickness time variation),
- to obtain the deposit cross-section profile in the z -direction at time t .

First experiments were performed with clay suspensions at a concentration of 1 g/l. Dead-end UF was performed at constant TMP (80 kPa) for a duration of 4 h. Feed suspension flowed from the bottom to the top of the channel and measurements were taken at 9 cm from the top of the channel height.

Figure 5 shows an example of the deposit thickness and permeate flux variations during filtration as a function of time. The initial flux is 204 l/h m^2 . It decreases rapidly during the first time period (from 0 to 25 min) and then more slowly until it reaches 20 l/h m^2 . The final cake thickness is $55 \mu\text{m}$ for a total deposited mass of 80 g/m^2 and a relative flux decrease of 87%. The strongest flux decrease corresponds to quite a small thickness between 0 and $10 \mu\text{m}$. The first layer is composed of a thin deposit with a high resistance. Above 25 min, the flux decrease is smaller whereas the deposit thickness varies from $10 \mu\text{m}$ to $55 \mu\text{m}$. The additional deposit is less resistant but thicker.

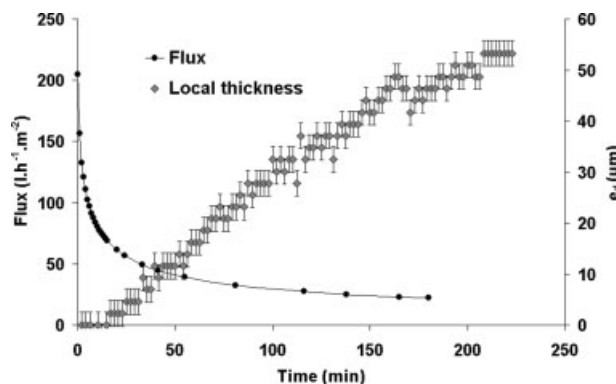


Figure 5. Deposit thickness and permeate flux variations for dead-end ultrafiltration of bentonite (TMP = 80 kPa, concentration = 1 g/l).

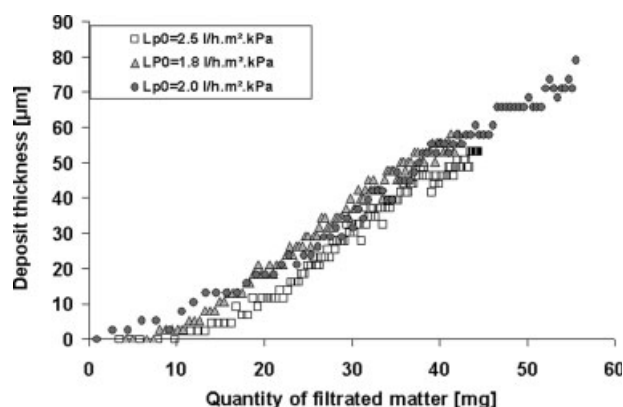


Figure 6. Deposit thickness vs the quantity of filtrated matter for three experiments (TMP = 80 kPa, concentration = 1 g/l).

L_{p0} is the initial permeability of the membrane (l/h m² kPa).

To assess the result reproducibility, three experiments were performed under the same operating conditions (TMP = 80 kPa, clay concentration = 1 g/l, feed from the bottom of the channel, measurements at 9 cm from the top of the channel height). Figure 6 shows the mean deposit thickness versus the quantity of filtrated matter for the three tests. For each experiment, a new membrane was used and the initial permeability was measured with pure water. Results reveal a good reproducibility concerning the mean deposit thickness value and the deposit growth dynamics with regard to the quantity of filtrated matter. The maximum percentage deviation of the data for the three replication runs from the average value is 8% which is reasonable.

Figure 7 is an example of deposit profile measurement calculated by dividing the channel into six transverse ROI for the three filtration runs for a deposited mass of 78 g/m². These results show that, at a given x -position, there are some significative cake thickness inhomogeneities along the channel width but no systematic confinement effect, in the transverse direction, was detected in our experiment. Moreover, the y -averaged cake thickness is similar for the three runs. The same observations remain valid when considering the same transverse cake thickness profiles but earlier in the fil-

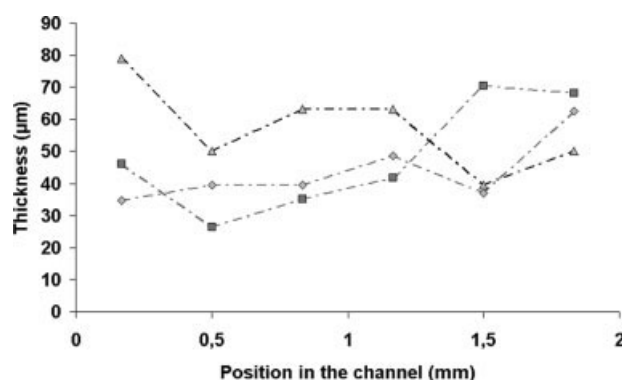


Figure 7. Deposit profile for the three experiments at 78 g/m² of deposited mass.

tration process (i.e. similar profiles but with lower thicknesses).

The integral of the profile curve on the channel width was estimated by calculating the area below the curve and compared to the integral for the mean thickness value, which was calculated in the same way assuming a homogeneous thickness in the y -direction. The comparison showed close agreement which proves the validity of the thickness profile measurement in the channel cross-section.

The results about the monitoring of the flux, deposit thickness, and profile show the capabilities of the method. First it is possible to follow the changes in the deposit structure with time and to distinguish several kinds of fouling layers. It is also possible to obtain the cross-section of the deposit and to see wall effects on the particle deposition.

Verification of the order of magnitude for thickness measurement: use of a simple filtration model

To validate the order of magnitude of the measured values of the deposit thickness, average thickness values were estimated using the classic cake filtration modeling at constant pressure considering clay particles as small flat plates with an equivalent diameter of 7 µm and a form factor of 1.8. The detailed principle of this model has been described elsewhere.¹⁸ This model assumes uniform and constant deposit properties on the membrane surface. The mean thickness (or global thickness) along the channel was computed using data (flow rate and TMP) from the experimental filtration curve.

Figure 8 shows the comparison between the global and local values for the same experiments as those plotted on Figure 6 (TMP = 80 kPa, clay concentration = 1 g/l, feed from the bottom of the channel, measurements at 9 cm from the top of the channel height). The comparison between measured and calculated values shows good agreement. The measured order of magnitude and cake growth dynamic is correct. For both cases, the global value overestimates the local measured thickness, especially at the beginning of the filtration. This could be due to a nonhomogeneous cake thickness along the x -direction deposit thickness distribution whereas calculated values assume a uniform deposit distribution on the membrane surface. In consequence, it would be interesting to use the optical method to study the nonuni-

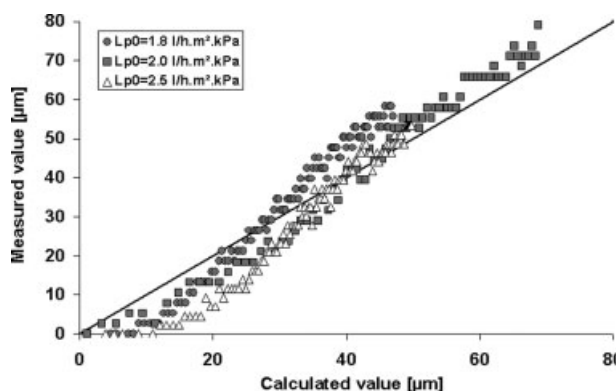


Figure 8. Comparison of measured and calculated deposit thickness (TMP = 80 kPa, concentration = 1 g/l).

formity of the deposit on the membrane. Moreover, it would be interesting to investigate the influence of the position of the feed alimentation (bottom of top of the channel) for a fixed x -position.

Conclusion and Future Applications of the Technique

In situ local characterization of cake formation is a key step toward a better understanding of filtration processes. Some noninvasive characterization methods have shown their efficiency for cake investigation on flat-sheet membrane. Few studies concern cake characterization in confined geometry like inside-out hollow-fiber membrane.

This study focuses on the development and the validation of a noninvasive characterization method applicable to a dead-end filtration deposit in a confined channel. This innovative method is based on the use of laser sheet at grazing incidence. It enables the deposit thickness at several locations in the vertical direction to be measured and the deposit thickness profile in the channel cross-section (z) to be obtained. Moreover, with this method it is possible to follow the deposit kinetics in relation to flow rate variations. First results were obtained with clay suspensions and show good reproducibility. The method could be limited by suspension concentration but in the range of tested concentrations (0–2 g/l), the signal is still fully usable. Experimental verification shows that the technique is useful for deposit thickness measurement ranging from 10 μm to hundreds of micrometers with a resolution of 3 μm . A further validation of the method will be assessed by comparing results with another characterization method in terms of deposit thickness under the same operating conditions.¹⁵

The use of this method as a tool for deposit characterization in dead-end UF in confined geometry is under investigation.¹⁹ In particular, the influence of operating conditions on deposit kinetics, deposit profile, and cake removal will be analyzed for different kinds of suspensions. This method can also be used at several locations on the fiber length to study the deposit spatial distribution. Thus, this developed method is a powerful characterization tool on a local scale that will enable a better understanding of fouling phenomena in dead-end UF. Indeed, it will be possible to investigate at lab-scale the influence of operating parameters (TMP, filtration and backwash runs, particles, etc.) on the deposit structure for an optimization of process performances.

Literature Cited

1. L  n   JM, Vial D, Moulart P. Status after 10 years of operation-overview of UF technology today. *Desalination*. 2000;131:17–25.

2. Remize PJ, Guigui C, Cabassud C. From a new method to consider backwash efficiency in surface water UF to the definition of remaining fouling. Proc. of MDIW-IWA Conference. L'Aquila, 2004.
3. Chen V, Li H, Fane AG. Non-invasive observation of synthetic membrane processes-a review of methods. *J Membr Sci*. 2004;241:23–44.
4. Chen JC, Li Q, Elimelech M. In situ monitoring techniques for concentration polarization and fouling phenomena in membrane filtration. *Adv Colloid Interface Sci*. 2004;107:83–108.
5. Li H, Fane AG, Coster HGL, Vigneswaran S. Direct observation of particle deposition on the membrane surface during crossflow microfiltration. *J Membr Sci*. 1998;149:83–97.
6. Mores WD, Davis RH. Direct visual observation of yeast deposition and removal during microfiltration. *J Membr Sci*. 2001;189:217–230.
7. Ferrando M, Rozek A, Zator M, Lopez F, G  ll C. An approach to membrane fouling characterization by confocal scanning laser microscopy. *J Membr Sci*. 2005;250:283–293.
8. Hamachi M, Mietton-Peuchot M. Experimental investigation of cake characteristics in crossflow microfiltration. *Chem Eng Sci*. 1999;54:4023–4030.
9. Tung KL, Wang SJ, Lu WM, Pan CH. In situ measurement of cake thickness distribution by a photointerrupt sensor. *J Membr Sci*. 2001;190:57–67.
10. Chung KY, Edelstein WA, Belfort G. Dean vortices with wall flux in a curved channel membrane system. VI. Two dimensional magnetic resonance imaging of the velocity field in a curved impermeable slit. *J Membr Sci*. 1993;81:151–162.
11. Wandelt B. Analyse de la formation des d  p  ts de particules lors d'un proc  d   d'ultrafiltration tangentielle. Visualisation par imagerie    r  sonance magn  tique nucl  aire. Institut National Polytechnique de Toulouse, 2003.
12. Wandelt B, Schmitz P, Houi D. Investigation of transient phenomena in crossflow microfiltration of colloidal suspensions using NMR microimaging. Sixth World Filtration Congress, Nagoya, Japan, 1993.
13. Pignon F, Magnin A, Piau JM, Cabane B, Aimar P, Meireles M, Lindner P. Structural characterization of deposits formed during frontal filtration. *J Membr Sci*. 2000;174:189–204.
14. Li J, Sanderson RD, Chai GY, Hallbauer DK. Development of an ultrasonic technique for in situ investigating the properties of deposited protein during crossflow ultrafiltration. *J Colloid Interface Sci*. 2005;284:228–238.
15. Mendret J, Guigui C, Cabassud C, Doubrovine N, Schmitz P, Duru P, Ferrandis JY, Laux, D. Development and comparison of optical and acoustic methods for in situ characterisation of particle fouling. *Desalination*. 2006;199:373–375.
16. Altmann J, Ripperger S. Particle deposition and layer formation at the crossflow microfiltration. *J Membr Sci*. 1997;124:119–128.
17. Schl  p T, Widmer F. Initial transient effects during cross-flow microfiltration of yeast suspensions. *J Membr Sci*. 1996;115:133–145.
18. Laborie S, Cabassud C, Durand-Bourlier L, L  n   JM. Flux enhancement by a continuous tangential gas flow in ultrafiltration hollow fibers for drinking water production: effects of slug flow on cake structure. *Filtr Sep*. 1997;34:887–891.
19. Mendret J, Guigui C, Cabassud C, Schmitz P. Dead-end ultrafiltration and backwash: dynamic characterisation of cake properties at local scale. *Desalination*. 2006;199:216–218.

Manuscript received Apr. 6, 2007, and revision received May 25, 2007.